NASA TECHNICAL MEMORANDUM

NASA TM X-2605

NASA TM X-2605

ANALYTICAL INVESTIGATION OF CONICAL DIFFUSERS

by James L. Means, Paul C. Glance, and Hugh A. Klassen

Lewis Research Center

and

U.S. Army Air Mobility R&D Laboratory

Cleveland, Ohio 44135

NATIONAL AERONAUTICS AND SPACE ADMINISTRATION • WASHINGTON, D. C. • AUGUST 1972

1. Report No.	2. Government Accession No.	3. Recipient's Catalog No.
NASA TM X-2605		

4. Title and Subtitle	5. Report Date
ANALYTICAL INVESTIGATION OF CONICAL DIFFUSERS	August 1972
	6. Performing Organization Code

7. Author(s)	8. Performing Organization Report No.
James L. Means, Paul C. Glance, and Hugh A. Klassen	E-6908
	10. Work Unit No. 132-15
9. Performing Organization Name and Address	11. Contract or Grant No.
NASA Lewis Research Center and U.S. Army Air Mobility R&D Laboratory Cleveland, Ohio 44135	
	13. Type of Report and Period Covered
12. Sponsoring Agency Name and Address	Technical Memorandum
National Aeronautics and Space Administration Washington, D.C. 20546	14. Sponsoring Agency Code

15. Supplementary Notes

16. Abstract

A study was made to determine if existing data for straight-channel single-plane divergence diffusers together with boundary-layer methods could be practically employed to predict conical diffuser performance in the high-speed flow regime. A semiempirical correlation technique, which uses the experimental performance of a straight-channel single-plane divergence diffuser, and a momentum integral boundary-layer method were employed to predict conical diffuser performance. Neither of these methods is applicable when the boundary layer separates. The momentum integral method was used to study the relative importance of various boundary layer parameters in correlating unstalled diffuser performance. Other investigators have found that the best diffuser performance occurs when the diffuser is operating in the transitory stall regime. Since the analytical methods presented in this report are not applicable after the point of boundary-layer separation, a criterion was established from examination of experimental tests which allows the designer to ascertain approximate diffuser performance in the transitory stall regime.

17. Key Words (Suggested by Author(s))		18. Distribution Statement
Diffuser	Turbomachinery	Unclassified - unlimited
Boundary-layer	Subsonic	
Fluid mechanics		

19. Security Classif. (of this report)	20. Security Classif. (of this page)	21. No. of Pages	22. Price*
Unclassified	Unclassified	26	$3.00

*For sale by the National Technical Information Service, Springfield, Virginia 22151

ANALYTICAL INVESTIGATION OF CONICAL DIFFUSERS

by James L. Means, Paul C. Glance, and Hugh A. Klassen

Lewis Research Center and
U. S. Army Air Mobility R&D Laboratory

SUMMARY

A study was made to determine if existing data for straight-channel single-plane divergence diffusers together with boundary-layer methods could be practically employed to predict conical diffuser performance in the high-speed flow regime. A semiempirical correlation technique, which uses the experimental performance of a straight-channel single-plane divergence diffuser, and a momentum integral boundary-layer method were employed to predict conical diffuser performance. Neither of these methods is applicable when the boundary layer separates. The momentum integral method was used to study the relative importance of various boundary parameters in correlating unstalled diffuser performance.

Other investigators have found that the best diffuser performance occurs when the diffuser is operating in the transitory stall regime. Since the analytical methods presented in this report are not applicable after the point of boundary-layer separation, a criterion was established from examination of experimental tests which allows the designer to ascertain approximate diffuser performance in the transitory stall regime.

INTRODUCTION

Recent investigations indicate that conical diffusers offer potential performance improvements in centrifugal compressors. At the present time, there is very little experimental or analytical data on the performance of conical diffusers for the high-speed flow conditions characteristic of centrifugal compressor diffusers. In this study (1) a semiempirical correlation method and (2) a boundary-layer technique were used to predict conical diffuser performance in the high-speed flow regime.

In the past, the flow in a diffuser has been analyzed by assuming that the diffuser flow can be approximated by a thin boundary layer adjacent to the wall and an inviscid core in the center of the passage. This type of flow is characteristic of the unstalled

flow regime. If the boundary layer separates from the wall, a region of transitory stall exists in which the separated region varies in position, size, and intensity with time. A jet flow regime is encountered when a steady-state separated region extends around the complete circumference of the diffuser and constricts the core flow to a jet in the center of the passage. Chang (ref. 1) provides an excellent discussion of the efforts to analyze unstalled diffusers. At the present time, there is no rigorous method of analyzing either the transitory stall regime or the jet flow regime.

Two analytical methods were employed to predict diffuser performance to the point of boundary-layer separation. After separation, a criterion which was developed from the examination of experimental data of conical diffusers, was used to predict diffuser performance. A discussion of the conical diffuser performance prediction methods is presented in this report together with an analytical study of the effect of inlet parameters upon unstalled diffuser performance.

METHOD OF ANALYSIS

Two analytical methods are described in this section. The first method, which is called the momentum integral method, divides the flow into two regimes, (1) an inviscid core and (2) a viscous boundary layer, and then solves the respective governing equations iteratively. The second method, which is called the semiempirical correlation technique, enables the employment of straight-wall plane diffuser data to predict the performance of conical diffusers. Neither of these methods is applicable after the point where the boundary layer separates. After separation, a criterion was employed to predict conical diffuser performance. This criterion was established from the examination of experimental conical diffuser data. The establishment of this criterion is discussed in this section.

Momentum Integral Method

The boundary-layer analysis was performed with the momentum integral technique developed by Sasman and Cresci (ref. 2) for turbulent compressible flow. This boundary-layer method is employed in the computer code of reference 3. This code was used, in the turbulent mode only and with the appropriate terms added to account for the three-dimensionality of the flow (see appendix B), to predict conical diffuser performance. The turbulent mode was used since compressor diffusers operate with a nonzero inlet blockage B_1 and a high turbulence level. All symbols are defined in appendix A.

In the momentum integral method the initial displacement and momentum thicknesses as well as edge conditions are needed in order to solve the boundary-layer problem. The displacement thickness δ^* was calculated from the inlet blockage (see eq. (D13)). If only the displacement thickness δ^* was specified, the momentum thickness θ could be estimated by assuming that the inlet shape factor $H \equiv \delta^*/\theta$ was the flat-plate value of 1.4. This enabled the computer code to start with the correct initial blockage and compute the boundary-layer development to the exit or to the point of boundary-layer separation. The interaction between the boundary layer and the inviscid core was used to determine the pressure gradient and boundary-layer edge velocity distribution throughout the diffuser. The inviscid core was computed from the one-dimensional, isentropic compressible flow relations (see appendix C). Separation of the boundary layer was determined by noting when the skin friction began to decrease rapidly toward zero. Once the flow separates, the boundary-layer model is no longer valid; therefore, only that part of the performance map that characterizes unstalled diffusers can be constructed with this method.

The calculation of the boundary layer for a given diffuser geometry was done in the following manner:

(1) The Mach number distribution along the edge of the boundary layer M_e was initially assumed to be constant through the diffuser. This enabled the boundary-layer program to calculate a schedule of displacement thicknesses for the boundary layer. By using this schedule of displacement thicknesses an effective area was calculated.

(2) A schedule of edge Mach numbers $\left(M_e^i\right)_{pr}$ was computed by using one-dimensional, isentropic compressible flow relations with an effective channel area, as discussed in appendix C.

(3) This edge Mach number was averaged with the previous guess for use in determining edge conditions for the i^{th} iteration

$$M_e^i = \frac{1}{2}\left[\left(M_e^i\right)_{pr} + M_e^{i-1}\right]$$

An average Mach number was used in this step instead of the predicted Mach number of step 2 because the Mach number of step 2 results in a pressure gradient that is too steep. This distribution of edge Mach numbers was then used to recalculate the schedule of displacement thickness for the diffuser.

(4) An edge Mach number schedule was recalculated in the manner described in step 2 and compared against the previous edge Mach number distribution of step 3. If the maximum error was greater than 0.1 percent, steps 3 and 4 were repeated. The iteration procedure was completed when the maximum error was equal to or less than 0.1 percent.

This procedure was used because the boundary-layer program proved to be sensitive to the edge Mach number. If the diffuser boundary layer is close to separation, the excessively adverse pressure gradient of step 2 causes the boundary-layer code to predict premature separation. Since the boundary-layer model is invalid where separation is predicted, an incorrect answer is obtained. Step 3 is necessary in order to avoid this problem.

Semiempirical Correlation Technique

This method enables the employment of two-dimensional plane diffuser data to predict conical diffuser performance. Given the geometry and experimental performance of a straight-channel single-plane divergence diffuser, these experimental data are used to predict the performance of an axisymmetric straight-wall conical diffuser. It is assumed that the performance of a straight-wall plane diffuser and a conical diffuser are equal when the following conditions are satisfied:

(1) The flow in the plane diffuser approaches a two-dimensional flow (i.e., the aspect ratio is large).

(2) The inlet and exit blockages, B_1 and B_2, of the two diffusers are equal.

(3) The inlet areas A_1 of the two diffusers are equal.

(4) The area ratios A_2/A_1 of the two diffusers are equal.

Also, it is assumed that there exists a transformation which permits the use of solutions of the straight-channel, single-plane divergence diffuser to derive solutions for the conical diffuser. This transformation is derived in reference 4.

These four conditions uniquely determine the geometry of the conical diffuser which has a performance C_{PR} identical to the experimental performance C_{PR} of the plane diffuser. Appendix D contains the derivation of the equations for determining the geometry of the conical diffuser corresponding to each plane diffuser.

The flow in a rectangular-cross-section diffuser approaches a two-dimensional flow as the aspect ratio AS of the diffuser approaches infinity. Thus, the straight-channel, single-plane divergence diffuser data used in the present technique were limited to plane diffusers possessing high aspect ratios. The experimental performance of straight-wall plane diffusers is reported in reference 5. The data in reference 5 have a maximum aspect ratio AS of 5. Therefore, these data (AS = 5) were employed in the present study to predict conical diffuser performance.

The present correlation technique assumes that the boundary layer is not separated. Therefore, this technique is limited to unstalled diffusers.

Diffuser Performance After Separation

Since boundary-layer methods fail after the point of boundary-layer separation, a rigorous analytical method of predicting the performance of diffusers operating in the transitory stall regime is not possible at the present time. A criterion for estimating conical diffuser performance after the point of boundary-layer separation will now be developed. Figure 1 depicts the diffuser pressure recovery effectiveness $\eta \equiv C_{PR}/(C_{PR})_{ideal}$ plotted as a function of dimensionless axial distance X/D_1. The point of boundary-layer separation, as predicted by the momentum integral method, is also shown on this figure. It has been observed experimentally that the effectiveness η

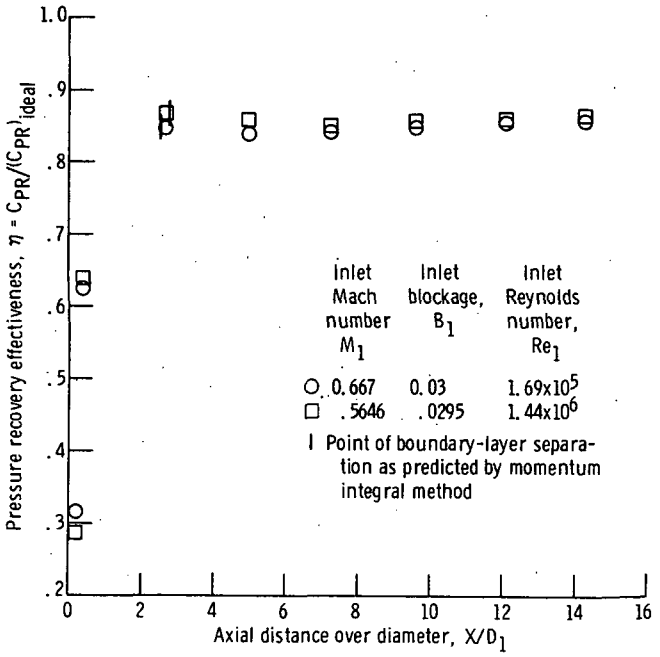

Figure 1. - Conical diffuser pressure recovery effectiveness based on wall pressure measurements. Cone angle, 8.09^0.

is approximately constant after the point of separation predicted by the momentum integral method.

Using the value of effectiveness predicted by the momentum integral method at separation as a constant enabled a reasonable prediction of the diffuser performance C_{PR} at the exit of the diffuser. That is, the following procedure gives a reasonable prediction of the performance of a conical diffuser operating in the transitory stall regime:

(1) The value of diffuser pressure recovery effectiveness at separation η_{sep} is

calculated by the momentum integral method.

(2) The pressure recovery C_{PR} after separation is then calculated from $C_{PR} = \eta_{sep}(C_{PR})_{ideal}$, where $(C_{PR})_{ideal}$ is the pressure recovery coefficient calculated when no boundary layer is present. This procedure is called the constant-effectiveness criterion in this report.

APPARATUS, INSTRUMENTATION, AND PROCEDURE

Predicted values of pressure recovery coefficient C_{PR} were compared with experimental values obtained from a conical diffuser with a cone angle of 8.09°. These tests were conducted at various values of inlet Mach number and Reynolds number.

Apparatus

The apparatus consisted of the test diffuser and an inlet and exhaust piping system with flow controls. The test diffuser is shown in figure 2. The diffuser consisted of

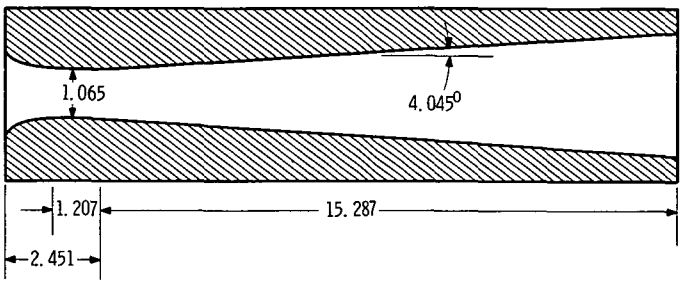

Figure 2. - Test diffuser. Area ratio, 9.143. Dimensions in centimeters.

a bellmouth inlet, a constant-diameter section, and the cone. The cone angle was 8.09°, throat diameter was 1.064 centimeters, and area ratio was 9.143.

A schematic drawing of the apparatus is shown in figure 3. Air to the nozzle passed through a flat-plate orifice, a remotely operated pressure control valve, and a tank before entering the nozzle. The tank was equipped with screens at the inlet and was installed to ensure a flat velocity profile upstream from the nozzle. Air from the nozzle was discharged through a remotely operated valve to the low-pressure exhaust system.

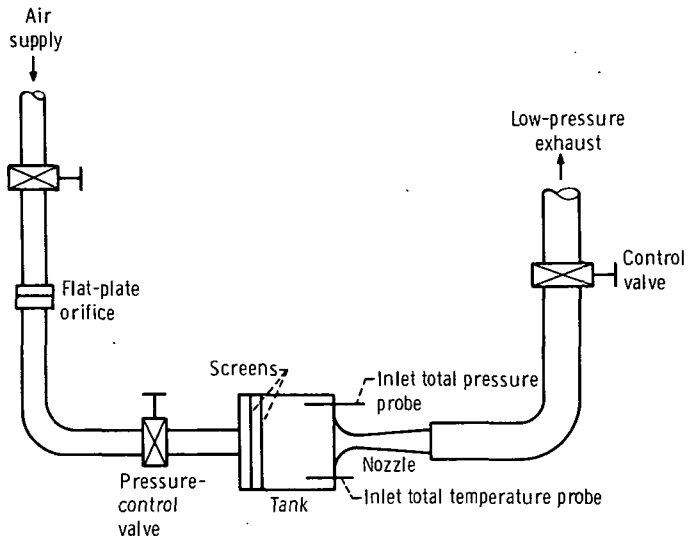

Figure 3. - Schematic of experimental equipment.

Instrumentation

Orifice and nozzle inlet temperatures were measured with copper-constantan thermocouples. Orifice pressures were measured with strain-gage transducers. Thermocouple and transducer outputs were read on a digital voltmeter. Mercury manometers were used to measure the inlet total and cone static pressures. In the throat section, where static pressure differences were small, water manometers were used to measure the pressure drop with respect to the upstream total pressure tap.

TABLE I. - STATIC PRESSURE

TAP LOCATIONS

(a) Throat-area taps

Tap	Distance from throat, cm (a)
1	-0.317
2	-.182
3	-.046
4	+.090
5	+.226
6	+.362
7	+.498
8	+.634

(b) Diffuser taps

Tap	Distance from throat, cm
1	0.65
2	2.95
3	5.38
4	7.82
5	10.26
6	12.95
7	15.24

[a] + denotes downstream; - denotes upstream.

There were 15 wall static pressure taps. Eight taps were in the vicinity of the throat. The remaining seven were used to measure pressure along the cone. These taps were spaced at intervals of 2.442 centimeters. Tap locations are shown in table I.

Procedure

All data were obtained with subsonic velocity throughout the diffuser. Inlet pressure was controlled by the upstream control valve. Velocity level was then adjusted with the downstream valve. Inlet air temperature was approximately 297 K.

RESULTS AND DISCUSSION

Analytical Methods

The comparison of the results from the semiempirical correlation technique with the results of the momentum integral method is given in figure 4. Figure 4 presents

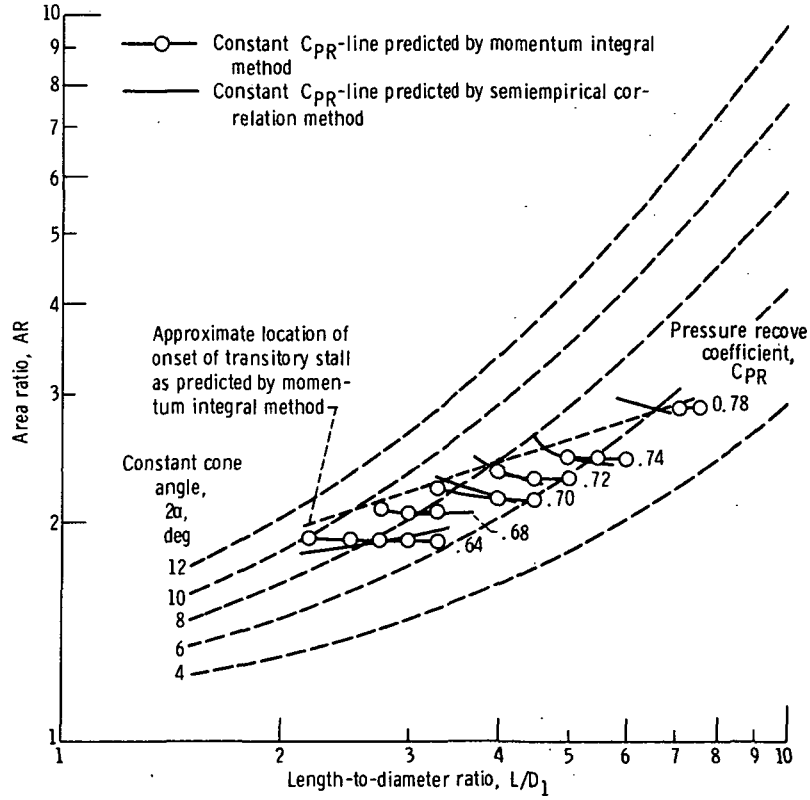

Figure 4. - Conical diffuser performance map. Inlet conditions: Mach number M_1, 0.2; blockage B_1, 0.02; Reynolds number Re_1, 161 000.

lines of constant pressure recovery C_{PR} as determined by both the momentum integral and semiempirical correlation methods as a function of area ratio AR and length-to-inlet-diameter ratio L/D_1. For convenience, lines of constant cone angle 2α are also shown in figure 4. The line of "onset of transitory stall," shown in figure 4, is the point at which the boundary layer separates at the diffuser exit as predicted by the momentum integral method. Since momentum integral boundary-layer techniques are inaccurate near the point of separation, the onset-of-transitory-stall line shown in figure 4 may not be an accurate estimate of the line dividing the transitory stall and unseparated flow regimes. The onset-of-transitory-stall line represents the limit of the applicability of boundary-layer methods. Above this line empirical or approximate methods must be employed in order to estimate diffuser performance. Examination of figure 4 reveals that conical diffuser performance improves as L/D increases.

Figures 5 to 7 depict the change in unstalled conical diffuser performance due to variations of inlet shape factor, inlet Reynolds number, and inlet blockage, respectively. The significance of the inlet shape factor H_1 was studied by plotting the pres-

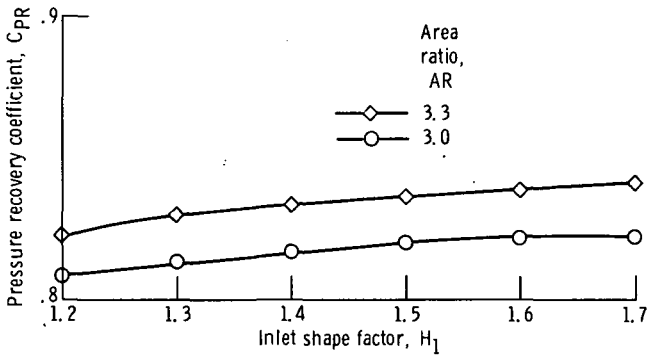

Figure 5. - Effect of initial shape factor on diffuser performance for unstalled conical diffusers. Inlet conditions: Mach number M_1, 0.2; blockage B_1, 0.02; length-to-diameter ratio L/D_1, 10.

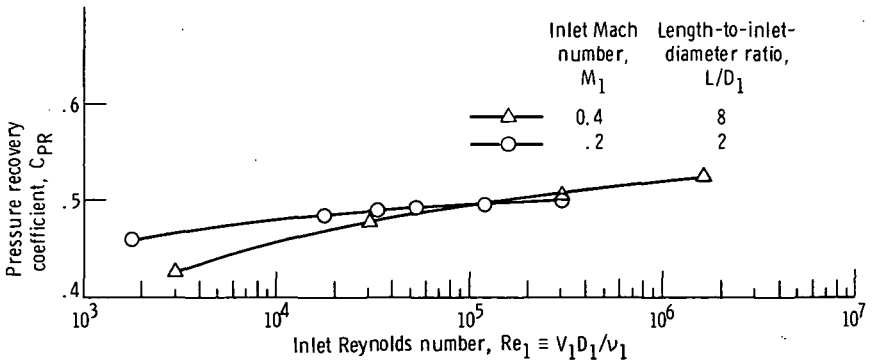

Figure 6. - Effect of Reynolds number variation on diffuser performance for unstalled conical diffusers. Inlet conditions: blockage B_1, 0.03; area ratio AR, 1.5.

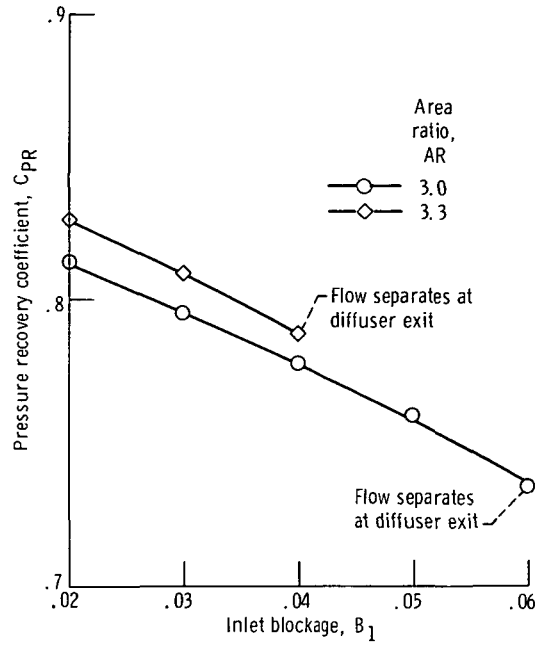

Figure 7. - Effect of inlet blockage on diffuser performance for unstalled conical diffusers. Inlet conditions: Mach number M_1, 0.2; shape factor H_1, 1.4; length-to-diameter ratio, 10.

sure recovery coefficient C_{PR} against H_1 with all other parameters held constant. The analysis indicated that the performance improved as the shape factor increased (fig. 5). This indicates that the diffuser may perform best when the initial boundary-layer shape factor is typical of flow in an adverse pressure gradient (i.e., $H_1 = 1.4$).

The significance of inlet Reynolds number Re_1 was studied by plotting C_{PR} against Re_1 with all other parameters held constant (fig. 6). The analysis indicated that performance improved slightly as the inlet Reynolds number increased, and thus the effect of inlet Reynolds number is secondary when compared to all other parameters. This conclusion applies only to unstalled conical diffusers.

The significance of inlet blockage B_1 was studied by plotting C_{PR} against B_1 with all other parameters held constant. The analysis indicated that diffuser performance is strongly dependent on inlet blockage (fig. 7). As the inlet blockage increased, diffuser performance decreased. The effects of inlet shape factor and Reynolds number are secondary when compared to the effect of blockage (figs. 5 to 7).

Comparison of Predicted and Experimental Results

The comparisons of the predicted and experimental results are shown in figures 8(a) and (b). These figures present the experimental and predicted pressure recovery C_{PR}

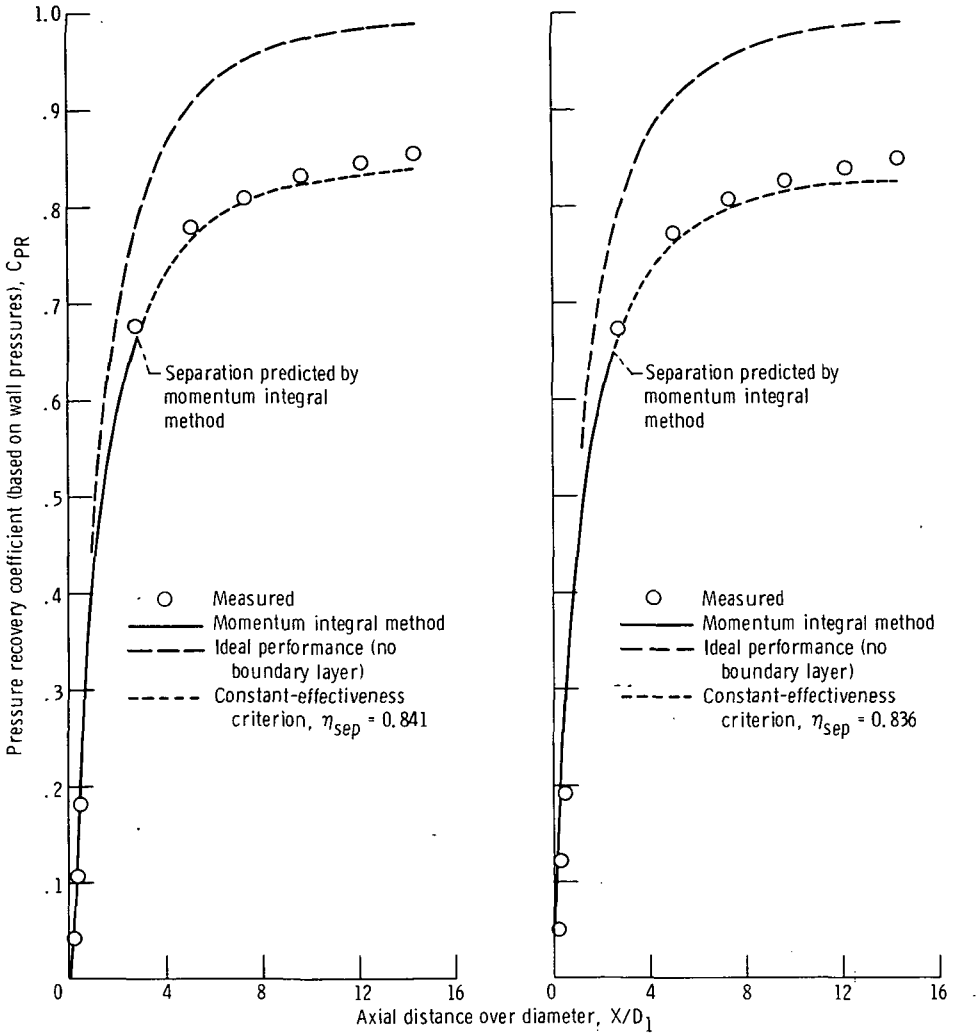

(a) Inlet conditions: wall Mach number $(M_1)_{wall}$, 0.5646; blockage B_1, 0.0295; Reynolds number Re_1, 1.44×10^5.

(b) Inlet conditions: wall Mach number $(M_1)_{wall}$, 0.667; blockage B_1, 0.03; Reynolds number Re_1, 1.69×10^5.

Figure 8. - Comparison of measured and predicted conical diffuser performance. Cone angle, 8.09^0.

plotted as a function of diffuser dimensionless length X/D_1 for various values of inlet Mach number and inlet blockage. The momentum integral method is employed to predict the pressure recovery to the point of boundary-layer separation. As shown in the figures, the momentum integral method is in good agreement with the experimental results.

After separation, it is assumed that the diffuser pressure recovery effectiveness η is constant and equal to the value of effectiveness at separation η_{sep}. As shown in figure 8, this criterion yields satisfactory results; that is, the agreement is within 3 percent at the diffuser exit for the two cases considered. Examination of 10 unpublished conical diffuser test results indicates that the pressure recovery effectiveness η is

constant to within 10 percent, after the point of separation predicted by the momentum integral method for cone angles less than 12° and subsonic inlet Mach numbers. Further experimental work needs to be conducted in order to improve and modify the constant-effectiveness criterion.

Conical Diffuser Design

The design of a diffuser is greatly facilitated by employment of performance maps similar to the map shown in figure 4. In the absence of experimental performance maps, performance maps can be estimated by plotting several values of predicted pressure recovery coefficient C_{PR}. The pressure recovery coefficient may be predicted by the methods described in the section METHOD OF ANALYSIS.

In general, increasing the length of a conical diffuser will improve its performance (fig. 4). However, the designer is usually limited to a finite volume into which the diffuser must fit. Therefore, the design problem is to find the conical diffuser possessing the largest pressure recovery (for a given set of inlet conditions M_1, B_1, and Re_1) which also lies within a prescribed volume envelope determined by a range of L/D_1 and AR values. A conical diffuser which satisfies these conditions is defined as the optimum conical diffuser.

A performance map, for the inlet conditions $M_1 = 0.5645$, $B_1 = 0.0295$, and $Re_1 = 1.438 \times 10^6$, has been generated by using the momentum integral method and the constant-effectiveness criterion and is shown in figure 9. The 8.09° conical diffuser test result ($C_{PR} = 0.855$), shown in figure 8(a), is also plotted in figure 9. There is a

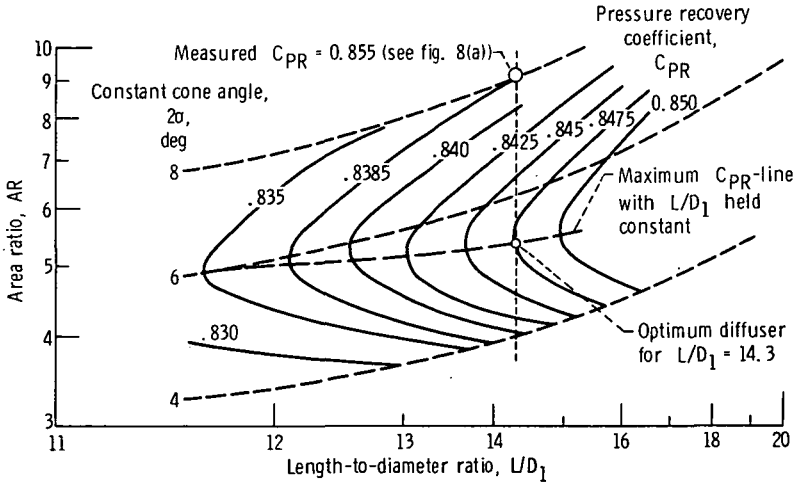

Figure 9. - Predicted conical diffuser performance map. Inlet conditions: Mach number M_1, 0.5646; blockage B_1, 0.0295; Reynolds number Re, 1.44×10^5; cone angle, 8.09°.

2 percent difference between the predicted (0.8385) and measured (0.855) pressure recovery coefficients. This 2 percent error is well within the accuracy of this prediction method. If it is assumed that the predicted map (fig. 9) gives a reasonable indication of how performance varies with geometry, the following conclusions can be made:

(1) Figure 9 suggests that the performance of the 8.09° conical diffuser can be bettered by using a 5.26° diffuser; that is, the optimum conical diffuser with a L/D_1 of 14.3 is a 5.26° diffuser.

(2) Figure 9 also suggests that the 8.09° diffuser can be replaced by a smaller diffuser (AR = 5.0, L/D_1 = 12.2) with no reduction in performance.

SUMMARY OF RESULTS

A study was made to determine if existing data for straight-channel, single-plane divergence diffusers together with boundary-layer methods could be employed to predict conical diffuser performance. The results of this study can be summarized as follows:

1. There is good general agreement between the momentum integral method and the semiempirical correlation method in the unstalled flow regime.

2. The agreement between the momentum integral method and experiments is good to the point of boundary-layer separation.

3. Examination of experimental data showed that the pressure recovery effectiveness is approximately constant after the point of boundary-layer separation predicted by the momentum integral method. This constant-effectiveness criterion was employed to predict conical diffuser performance after separation, and the agreement with experiment was satisfactory for the cases investigated. Further experimental work needs to be conducted in order to modify and improve this criterion.

4. The effects of the boundary-layer inlet shape factor and inlet Reynolds number are secondary when compared to the effects of inlet blockage, area ratio, length-to-diameter ratio, and inlet Mach number upon unstalled conical diffuser performance.

Lewis Research Center,
National Aeronautics and Space Administration,
and
U.S. Army Air Mobility R&D Laboratory,
Cleveland, Ohio, May 4, 1972,
132-15.

APPENDIX A

SYMBOLS

A	cross-sectional area, m^2
A_e	effective area, m^2
A_u	unblocked area (figs. 12 and 13), m^2
AR	area ratio, A_2/A_1
AS	aspect ratio, W/Y_1
B	blockage (dimensionless), $1 - (A_e/A)$
C_{PR}	pressure recovery coefficient (dimensionless), $(P_2 - P_1)/(P_1' - P_1)$
$(C_{PR})_{ideal}$	pressure recovery coefficient calculated when no boundary layer is present
D	diameter, m
D_H	hydraulic diameter, m
H	shape factor (dimensionless), δ^*/θ
L	axial length of diffuser, m
M	Mach number (dimensionless)
M_e	Mach number at boundary-layer edge
n	exponent (eq. (D22))
P	pressure, N/m^2
P'	total pressure, N/m^2
R	radius, m
Re	Reynolds number (dimensionless), VD_H/ν
S	length of diffuser wall, m
u_∞	free-stream fluid velocity, m/sec
V	velocity, m/sec
W	width of plane diffuser, m
X	running axial length of diffuser, m
Y	height of plane diffuser, m
α	angle between diffuser wall and axial direction, deg

γ ratio of specific heats

δ^* displacement thickness of boundary layer, m

$\Delta\delta^*$ growth of displacement thickness, $\delta_2^* - \delta_1^*$, m

η pressure recovery effectiveness (dimensionless), $C_{PR}/(C_{PR})_{ideal}$

θ momentum thickness, m

ν viscosity, m^2/sec

ξ running length of diffuser wall (fig. 11), m

Subscripts:

p straight-channel, single-plane, divergence diffuser

pr predicted results

1 inlet cross section

2 exit cross section

sep point of boundary-layer separation

wall diffuser wall

Superscripts:

i step in iteration procedure

* sonic conditions

APPENDIX B

AXISYMMETRIC BOUNDARY-LAYER EXTENSION

McNally's computer code (ref. 3) was used to compute the turbulent boundary-layer development in conical diffusers. McNally's code implements Sasman and Cresci's momentum integral technique but omits the terms necessary to calculate boundary layers in an axisymmetric flow. In order to extend McNally's code to include axisymmetric flows, equation (8) of reference 3 should be amended to read

$$\frac{df}{d\xi} = 1.268\left\{\frac{-f}{M_e}\frac{dM_e}{d\xi}\left[1+(1+S_W)H_i\right] - \frac{jf}{R}\frac{dR}{d\xi} + A\right\}$$

where ξ is the coordinate parallel to the body surface in the streamwise direction (this variable is labeled x in ref. 3), M_e is the edge Mach number, and R is the radius of the body. The variables A, H_i, S_W, and f are defined in reference 3, and

$$j = \begin{cases} 1 & \text{axisymmetric flow} \\ 0 & \text{planar flow} \end{cases}$$

With this modification, the code of reference 3 was used to predict the boundary-layer development in conical diffusers.

APPENDIX C

INVISCID CORE MODEL

Isentropic, one-dimensional flow was used to model the inviscid core. The interaction between the boundary layer and the inviscid core was accounted for by using an effective area A_e

$$A_e = \pi\left[R - \delta^*(\xi)\right]^2$$

to compute the Mach number in the core. Therefore, at a given station the core Mach number is found by solving the equation

$$M_e^2\left(\frac{A_e}{A^*}\right)^2 - \left[\frac{2}{\gamma+1}\left(1 + \frac{\gamma-1}{2}M_e^2\right)\right]^{(\gamma+1)/(\gamma-1)} = 0$$

for the Mach number M_e. The solution of this equation for each A_e/A^* yields a schedule of M_e as a function of ξ. This schedule was used in the iteration procedure to determine the diffuser performance.

APPENDIX D

DERIVATION OF EQUATIONS USED IN SEMIEMPIRICAL METHOD

This section contains the derivation of the equations used in the semiempirical method to determine the geometry of the conical diffuser corresponding to each plane diffuser. The five assumptions listed in the method of analysis are employed in the following derivation.

A straight-wall plane diffuser and a straight-wall conical diffuser are shown in figures 10 and 11, respectively. The inlet areas A_1, the exit and inlet blockages B_2 and B_1, and the area ratios A_2/A_1 of the two diffusers are each constrained to be equal.

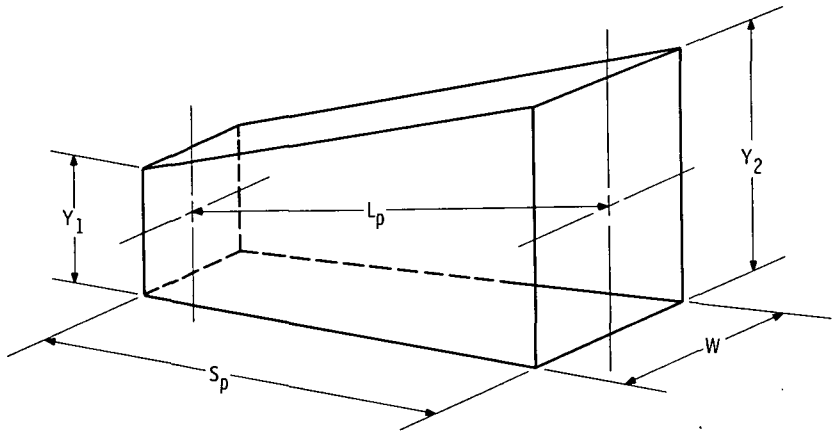

Figure 10. - Straight-wall plane diffuser.

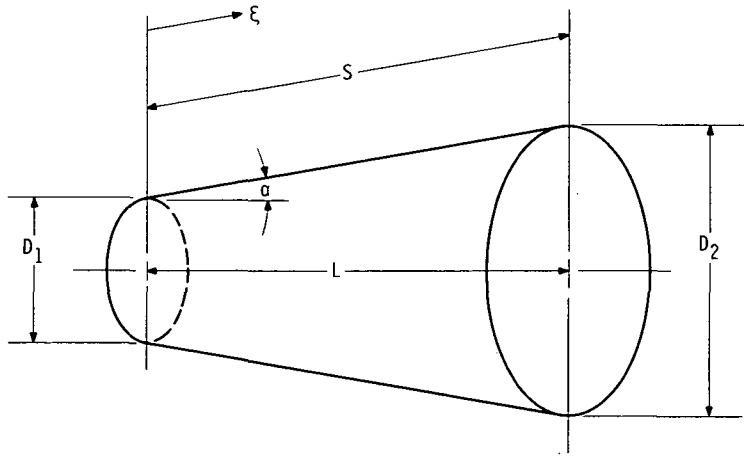

Figure 11. - Straight-wall conical diffuser.

The aspect ratio AS of the plane diffuser is defined as

$$AS = \frac{W}{Y_1} \tag{D1}$$

Solving for the width W of the plane diffuser yields

$$W = Y_1(AS) \tag{D2}$$

The area ratio A_2/A_1 of the plane diffuser is defined as

$$\frac{A_2}{A_1} = \frac{Y_2 W}{Y_1 W} \tag{D3}$$

or

$$Y_2 = \frac{A_2}{A_1} Y_1 \tag{D4}$$

Equation (D5) follows immediately from the geometry of figure 10:

$$S_p^2 = L_p^2 + \frac{1}{4}(Y_2 - Y_1)^2 \tag{D5}$$

Substituting equation (D4) into equation (D5) yields

$$S_p^2 = \left(\frac{Y_1}{2}\right)^2 \left(\frac{A_2}{A_1} - 1\right)^2 + L_p^2 \tag{D6}$$

Equating the inlet areas A_1 of the two diffusers yields

$$Y_1 W = \frac{\pi}{4} D_1^2 \tag{D7}$$

Substituting equation (D2) into equation (D7) and solving for D_1^2 yields

$$D_1^2 = \frac{4}{\pi} Y_1^2 (AS) \tag{D8}$$

which determines the inlet diameter D_1 of the conical diffuser.

Equating the area ratios A_2/A_1 of the two diffusers yields

$$\frac{Y_2 W}{Y_1 W} = \frac{\frac{\pi}{4} D_2^2}{\frac{\pi}{4} D_1^2} = \frac{A_2}{A_1} \tag{D9}$$

or

$$D_2 = \sqrt{\frac{Y_2}{Y_1}}\, D_1 = \sqrt{\frac{A_2}{A_1}}\, D_1 \tag{D10}$$

which determines the exit diameter D_2 of the conical diffuser. Equation (D11) follows immediately from the geometry of figure 11:

$$S^2 = L^2 + \left(\frac{D_2 - D_1}{2}\right)^2 \tag{D11}$$

The "effective areas" A_e are defined as the crosshatched areas shown in figures 12 and 13.

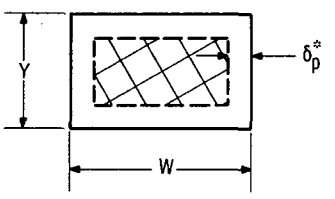

Figure 12. - Affected area of straight-channel, single-plane divergence diffuser. $(A_e)_p \equiv (W - 2\delta_p^*)(Y - 2\delta_p^*)$.

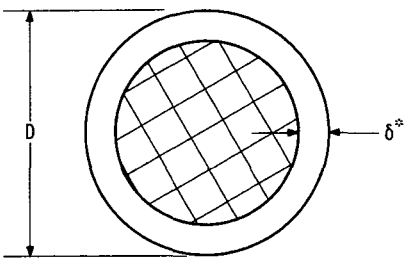

Figure 13. - Affected area of conical divergence diffuser. $A_e \equiv \pi\left(\frac{D}{2} - \delta^*\right)^2$.

The blockage B is defined as 1 minus the ratio of the effective area A_e to the geometric area A, that is,

$$B \equiv 1 - \frac{A_e}{A} \tag{D12}$$

Substituting the definitions of A and A_e for the conical diffuser into equation (D12) yields

$$B = 1 - \frac{\pi\left(\frac{D}{2} - \delta^*\right)^2}{\frac{\pi}{4} D^2} \tag{D13}$$

or

$$\delta^* = \frac{D}{2}\left(1 - \sqrt{1 - B}\right) \tag{D14}$$

Substituting the definitions of A and A_e for the plane diffuser into equation (D12) yields

$$B = \frac{1 - (W - 2\delta_p^*)(Y - 2\delta_p^*)}{YW} \tag{D15}$$

or

$$4(\delta_p^*)^2 - 2(W + Y)\delta_p^* + YWB = 0 \tag{D16}$$

Solving for δ_p^* yields

$$\delta_p^* = \frac{1}{4}(W + Y) - \frac{1}{4}\left[(W + Y)^2 - 4YWB\right]^{1/2} \tag{D17}$$

The growth of the boundary-layer displacement thickness $\Delta\delta^*$ is defined as the exit thickness minus the inlet thickness, that is,

$$\Delta\delta^* \equiv \delta_2^* - \delta_1^* \tag{D18}$$

The inlet blockage B_1 is given with the experimental data reported in reference 5. The inlet Mach number M_1 and exit pressure ratio P_2/P are given in reference 5. The exit blockage B_2 can be calculated in the following manner:

$$B_2 = 1 - \frac{\left(\frac{A_2}{A^*}\right)_{effective}}{\left(\frac{A_2}{A^*}\right)_{isentropic}} \tag{D19}$$

where the effective area ratio $(A_2/A^*)_{effective}$ is given in reference 7 as

$$\left(\frac{A_2}{A^*}\right)_{effective} = \frac{\sqrt{\frac{\gamma - 1}{2}}\left(\frac{2}{\gamma + 1}\right)^{(\gamma+1)/(2\gamma-2)}}{\sqrt{1 - \left(\frac{P_2}{P'}\right)^{(\gamma-1)/\gamma}}\left(\frac{P_2}{P'}\right)^{1/\gamma}} \tag{D20}$$

and the isentropic area ratio $(A_2/A^*)_{isentropic}$ is given in reference 6 as

$$\frac{\frac{A_2}{A_1}}{\frac{A_1}{A^*}} = \frac{A_2}{A_1}\frac{1}{M_1}\left[\frac{2}{\gamma + 1}\left(1 + \frac{\gamma - 1}{2}M_1^2\right)\right]^{-(\gamma+1)/2(\gamma-1)} \tag{D21}$$

The isentropic area ratio is the area ratio at zero blockage. The transformation which permits the use of solutions of a plane diffuser to be used to derive solutions for a conical diffuser is given by equation (60) of reference 4, which is given here (with δ^* and δ_p^* replaced by $\Delta\delta^*$ and $\Delta\delta_p^*$, respectively)

$$\frac{\Delta\delta_p^*}{S_p}\left(\frac{u_\infty S_p}{\nu_\infty}\right)^{n/(n+1)} = \frac{\Delta\delta^*}{S}\left(\frac{u_\infty S}{\nu_\infty}\right)^{n/(n+1)}\left\{\frac{\frac{S}{S}\left(\frac{D_2}{2S}\right)^{n+1}}{\int_0^1 \left[\frac{D(\xi)}{2S}\right]^{n+1} d\left(\frac{\xi}{S}\right)}\right\}^{1/(n+1)} \tag{D22}$$

or

$$\Delta\delta_p^*(S_p)^{-1/(n+1)} = \Delta\delta^*(S)^{-1/(n+1)} \frac{D_2}{2S} \left\{ \int_{\xi/S=0}^{1} \left[\frac{D(\xi)}{2S}\right]^{n+1} d\left(\frac{\xi}{S}\right) \right\}^{-1/(n+1)} \tag{D23}$$

Substituting $D(\xi) = D_1 + 2\xi \sin \alpha$ (fig. 11) into equation (D23), integrating, and cancelling yields

$$\Delta\delta_p^*(S_p)^{-1/(n+1)} = \Delta\delta^*(S)^{-1/(n+1)} \frac{D_2}{2S} \left[\frac{\left(\frac{D_1}{2S} + \sin \alpha\right)^{n+2}}{(n+2) \sin \alpha} \right]^{-1/(n+1)} \tag{D24}$$

Substituting $\sin \alpha = (D_2 - D_1)/2S$ into equation (D24) yields

$$\Delta\delta_p^*(S_p)^{-1/(n+1)} = \Delta\delta^*(S)^{-1/(n+1)} D_2 \left[\frac{D_2^{n+2}}{(n+2)(D_2 - D_1)} \right]^{-1/(n+1)} \tag{D25}$$

or

$$S = \left(\frac{\Delta\delta_p^*}{\Delta\delta^*}\right)^{-(n+1)} \frac{S_p(n+2)(D_2 - D_1)}{D_2} \tag{D26}$$

Substituting equation (D11) into equation (D26) and solving for L yields

$$L = \left[\left(\frac{\Delta\delta_p^*}{\Delta\delta^*}\right)^{-2(n+1)} S_p^2 (n+2)^2 \left(\frac{D_2 - D_1}{D_2}\right)^2 - \left(\frac{D_2 - D_1}{2}\right)^2 \right]^{1/2} \tag{D27}$$

The procedure for determining the geometry of the conical diffuser (D_1, D_2, and L) is summarized by the following steps:

(1) Y_1, A_2/A_1, AS, B_1, P_2/P', and M_1 are known for a straight-wall plane diffuser (assume n = 1).

(2) Calculate

$(A_2/A^*)_{effective}$ (eq. (D20))

$(A_2/A^*)_{isentropic}$ (eq. (D21))

B_2 (eq. (D19))

W (eq. (D2))

Y_2 (eq. (D4))

D_1 (eq. (D8))

D_2 (eq. (D10))

δ^* (eq. (D14))

δ_p^* (eq. (D17))

$\Delta\delta_p^*$ (eq. (D18))

$\Delta\delta^*$ (eq. (D18))

L (eq. (D27))

(3) These calculations determine the geometry of the conical diffuser (D_1, D_2, and L) which has a performance identical to the straight-wall plane diffuser of step 1.

REFERENCES

1. Chang, Paul K.: Separation of Flow. Pergamon Press, 1970, pp. 158-176.
2. Sasman, Philip K.; and Cresci, Robert J.: Compressible Turbulent Boundary Layer With Pressure Gradient and Heat Transfer. AIAA J., vol. 4, no. 1, Jan. 1966, pp. 19-25.
3. McNally, William D.: Fortran Program for Calculating Compressible Laminar and Turbulent Boundary Layers in Arbitrary Pressure Gradients. NASA TN D-5681, 1970.
4. Tetervin, Neal: A Generalization to Turbulent Boundary Layers of Mangler's Transformation Between Axisymmetric and Two-Dimensional Laminar Boundary Layers. Rep. NOLTR 69-47, Naval Ordnance Lab. (AD-692378), June 12, 1969.
5. Runstadler, Peter W. Jr.: Pressure Recovery Performance of Straight-Channel, Single-Plane Divergence Diffusers at High Mach Numbers. Rep. N-88, Creare, Inc. (USAAVLABS-TR-69-56, AD-865300), Oct. 1969.
6. Liepmann, H. W.; and Roshko, A.: Elements of Gasdynamics. John Wiley & Sons, Inc., 1957.

NATIONAL AERONAUTICS AND SPACE ADMISTRATION
WASHINGTON, D.C. 20546

OFFICIAL BUSINESS
PENALTY FOR PRIVATE USE $300

FIRST CLASS MAIL

POSTAGE AND FEES PAID
NATIONAL AERONAUTICS AND
SPACE ADMINISTRATION

U.S.MAIL

NASA 451

POSTMASTER: If Undeliverable (Section 158 Postal Manual) Do Not Return

"The aeronautical and space activities of the United States shall be conducted so as to contribute . . . to the expansion of human knowledge of phenomena in the atmosphere and space. The Administration shall provide for the widest practicable and appropriate dissemination of information concerning its activities and the results thereof."

—NATIONAL AERONAUTICS AND SPACE ACT OF 1958

NASA SCIENTIFIC AND TECHNICAL PUBLICATIONS

TECHNICAL REPORTS: Scientific and technical information considered important, complete, and a lasting contribution to existing knowledge.

TECHNICAL NOTES: Information less broad in scope but nevertheless of importance as a contribution to existing knowledge.

TECHNICAL MEMORANDUMS: Information receiving limited distribution because of preliminary data, security classification, or other reasons.

CONTRACTOR REPORTS: Scientific and technical information generated under a NASA contract or grant and considered an important contribution to existing knowledge.

TECHNICAL TRANSLATIONS: Information published in a foreign language considered to merit NASA distribution in English.

SPECIAL PUBLICATIONS: Information derived from or of value to NASA activities. Publications include conference proceedings, monographs, data compilations, handbooks, sourcebooks, and special bibliographies.

TECHNOLOGY UTILIZATION PUBLICATIONS: Information on technology used by NASA that may be of particular interest in commercial and other non-aerospace applications. Publications include Tech Briefs, Technology Utilization Reports and Technology Surveys.

Details on the availability of these publications may be obtained from:

SCIENTIFIC AND TECHNICAL INFORMATION OFFICE

NATIONAL AERONAUTICS AND SPACE ADMINISTRATION

Washington, D.C. 20546